Romanian Journal of Petroleum & Gas Technology
Vol. VI (LXXVII) • No. 2/2025

NUMERICAL MODELING OF CONVECTIVE AND MOLECULAR TRANSPORT MECHANISMS OF HYDROGEN IN DEPLETED GAS RESERVOIRS

Rami Doukeh [1], Timur-Vasile Chiș [1], Laura-Ștefania Păun [1], Alexandra Mohanu [1], Mihai Adrian Albulescu [1], Doru Bogdan Stoica [1*]

[1] Department of Well Drilling, Extraction and Transport of Hydrocarbons, Petroleum-Gas University of Ploiesti, 39 Bucharest Blvd., 100680 Ploiesti, Romania
* email (corresponding author): dstoica@upg-ploiesti.ro

DOI: 10.51865/JPGT.2025.02.15

ABSTRACT

This study presents a numerical investigation of hydrogen injection and migration in a depleted natural gas reservoir, integrating convective and molecular transport mechanisms. A 2D simulation model based on real geological data was developed using a discretized mesh and realistic operational parameters, including 15 active injection wells each delivering 250,000 Sm^3/day. Four main operational scenarios were analyzed: continuous injection over 120 days and three subsequent cycles incorporating post-injection relaxation intervals of 5, 10, and 15 days.

Results show that continuous injection leads to stable reservoir behavior, with progressive pressure buildup and efficient gas accommodation. However, the introduction of relaxation periods reveals improved gas redistribution and saturation homogeneity, especially in the 15-day case, where hydrogen diffusion becomes significantly more uniform across the reservoir volume. Despite minimal differences in global pressure between relaxation scenarios, only the extended relaxation phase ensures optimal pore space utilization and mitigates localized overpressure risks.

These findings emphasize the critical role of tailored injection-relaxation cycles in maximizing hydrogen storage efficiency and maintaining reservoir integrity, contributing to the optimization of underground hydrogen storage strategies in depleted gas formations.

Keywords: hydrogen storage, simulation, reservoir, gas wells, hydrogen transport mechanisms

INTRODUCTION

Underground hydrogen storage (UHS) systems are governed by complex hydrodynamic phenomena such as gas mixing and trapping, lateral dispersion of hydrogen (H_2), and viscous fingering all strongly influenced by capillary pressure hysteresis and relative permeability. These transport behaviors are inherently dependent on rock and fluid-specific parameters, including geological structure, porosity, permeability, viscosity, capillary forces, and fluid densities [1-4].

Recent modeling efforts have largely focused on simulating these hydrodynamic aspects to evaluate the viability and operational safety of UHS in porous reservoirs. A variety of reservoir simulation platforms including DuMux [5-7], Eclipse [8,9], TOUGH2-PetraSim [10,11], CMG-GEM [12,13], and COMSOL Multiphysics [14,15] have been employed to assess hydrogen transport mechanisms under realistic subsurface conditions. Additionally, machine learning (ML) tools are emerging to augment predictive capabilities through data-driven calibration [16].

Lysyy et al. [17] applied the Eclipse 100 simulator to assess H_2 storage in the Norne oil and gas field (Norway), demonstrating recovery efficiencies up to 87% in gas zones, while oil and water zones yielded 49% and 77%, respectively. Their study highlighted the dual role of formation gas as both a cushion and a diluent, with gas mixing adversely affecting the recovered hydrogen purity.

Pfeiffer and Bauer extended this approach using Eclipse 300, simulating UHS in Northern Germany. Their results underscored the evolution of system performance over multiple storage cycles, with cumulative energy delivery exceeding 20% of the projected scenario demand. Optimization of injection schemes—such as intermittent stoppages to enhance injectivity was proposed to further improve storage efficiency [18].

Luboń and Tarkowski employed PetraSim coupled with TOUGH2 to model seasonal hydrogen injection-recovery cycles in the Suliszewo structure. Their findings indicated that maintaining constant injection and withdrawal rates (up to 3 kg/s) under pressure constraints could enable long-term stability and high recovery efficiency across repeated cycles [10].

Mahdi et al. [19] used TOUGH2 with the EWASG equation of state to simulate hydrogen migration in a heterogeneous sandstone reservoir. They concluded that elevated injection rates, in the absence of an effective caprock, lead to hydrogen leakage and increased gas fingering effects.

Jadhawar and Saeed, using the CMG-GEM platform, explored the influence of injection/production dynamics, cycle frequency, and downtime intervals [20]. Their research revealed that high-frequency cycling and moderate injection rates yield superior recovery, while extended cycles and minimal downtime promote gas dispersion and reduce retrieval efficiency. Deploying multiple wells further enhanced system performance by equalizing pressure distribution and mitigating localized pressure build-up or depletion [20].

Overall, these advanced modeling studies offer critical insights into the optimization of hydrogen injection-recovery strategies, the minimization of transport-related losses, and the design of efficient, cyclic storage protocols in depleted gas reservoirs.

This study serves as an applied extension of the theoretical foundations outlined in recent literature, presenting a detailed numerical analysis of hydrogen injection and transport behavior in a depleted gas reservoir. The focus was placed on the interaction between convective flow, molecular diffusion, and pressure redistribution under a range of operational scenarios. Both continuous injection and cyclic injection-relaxation schemes were simulated using real geological and field data to reflect practical underground hydrogen storage conditions.

The simulation results strongly align with the hydrodynamic behaviors predicted in the introduction, particularly those governed by pressure hysteresis and heterogeneity in porous media properties. The findings underscore that carefully calibrated relaxation

intervals play a critical role in facilitating pressure equilibrium and enhancing gas saturation distribution within the reservoir. This direct correlation between theoretical modeling and numerical outcomes reinforces the importance of developing dynamic injection strategies that incorporate structured injection–pause cycles to ensure system stability and long-term storage efficiency.

METHODOLOGY

To conduct this study, essential data were collected regarding the average characteristics of the reservoir, including initial pressure, gas cushion volume, seasonal injection rates, and average durations for both storage and equilibrium phases. These parameters served as the foundation for comprehensive numerical simulations and subsequent analyses, aimed at assessing the hydrogen injection process under optimal and efficient operating conditions. The economic operator provided actual data on the gas mixture composition in the reservoir (gas cushion) by submitting chromatographic analysis reports, which were instrumental in accurately identifying the gas properties and component distribution.

The total storage capacity of the underground natural gas facility was approximately 300 million Sm^3, with a maintained initial reservoir pressure of 30 bar. The simulation model was constructed based on the geological architecture of the reservoir and discretized into a mesh comprising approximately 16,000 cells [21,22]. Structurally, the reservoir exhibits the shape of an elongated dome oriented from northwest to southeast, with a relatively uniform depth and gentle slope. Treated as a homogeneous hydrodynamic unit, the reservoir features a well-defined vertical saturation threshold located along the 900 meter isobath, as depicted in Figure 1.(a).

Petrophysical analyses of the reservoir rock indicated porosity values ranging between 20% and 26%, consistent with regional porosity maps. The permeability values ranged from 10 to 70 millidarcies, with representative values of 10 millidarcies for permeability and 20% for porosity selected for simulation purposes. Under these conditions, overpressure effects were observed to be more pronounced near the injection wells, gradually decreasing toward the reservoir boundaries.

H_2 Storage simulation model was developed using a two-dimensional (2D) numerical framework The based on the actual geometry of a flat-type depleted gas reservoir, where the formation thickness is relatively uniform. As illustrated in Figure 1.(b), the model incorporates the spatial layout of 15 existing and proposed wells that may be partially or fully operational during the hydrogen storage phase. To investigate hydrogen migration behavior, several cyclic injection scenarios were simulated using real field data, considering both continuous injection and periodic relaxation intervals of 5, 10, and 15 days.

In order to clearly assess reservoir performance under uniform injection conditions, it was assumed that all 15 wells inject hydrogen at an equal rate of 250,000 Sm^3/day, as shown in Figure 1.(b). The initial pressure was set at 30 bar and considered homogeneous across the entire reservoir domain. This modeling approach allowed for an integrated evaluation of convective and diffusive hydrogen transport processes within a realistic geological framework.

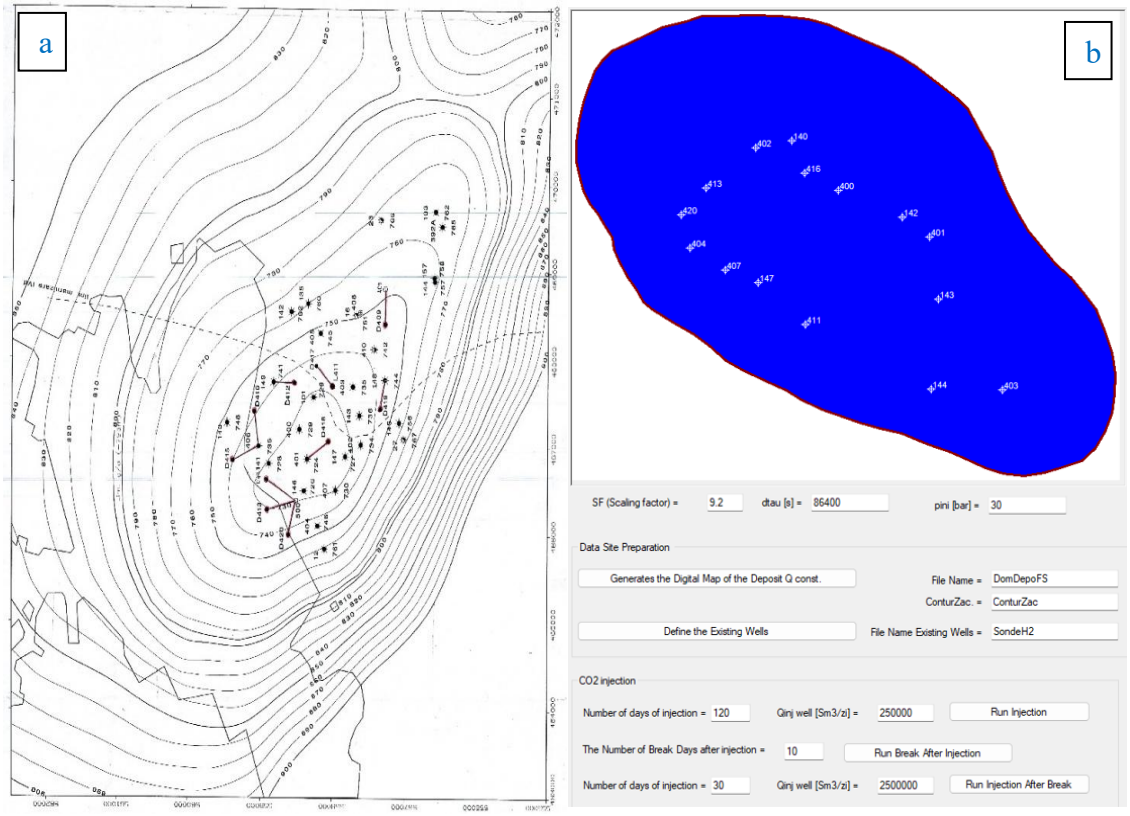

***Figure 1**. (a) Structural isobath map of the gas reservoir – reservoir morphology and distribution of productive wells (Gligor A.M., Contributions regarding the optimization of the energy-related processes for storing natural gas, Petroleum-Gas University of Ploiesti, Doctoral Thesis, 2014); (b) Outline of the reservoir's domain of interest, well distribution, and data input configuration within the simulation model*

MATHEMATICAL MODEL AND INTEGRATION CONDITIONS FOR GAS FLOW IN POROUS MEDIA

To simulate gas transport phenomena within a horizontal porous medium, flow equations were formulated in Cartesian coordinates. The two-dimensional gas migration under uniform pressure is governed by Darcy's law, the continuity equation, and the real gas equation of state, as detailed in prior studies [21,22].

The Du Fort Frankel method [23,24] was employed due to its unconditional stability and reliance on two preceding time steps ideal for modeling dynamic reservoir behavior. Its finite difference implementation allows accurate pressure field evaluation across a discretized domain. However, due to its dependence on two prior states, an explicit method was adopted at critical steps, allowing forward calculation from a single preceding time point.

Numerical integration requires the definition of initial and boundary conditions. Initial parameters—such as pressure and gas volume are set to mimic the onset of hydrogen injection, assuming uniform initial pressure. Two boundary condition types are considered: external and wellbore. For injection blocks, the hydrogen pressure superimposes on the existing reservoir pressure, raising the bottomhole pressure. In depleted reservoirs, external boundaries are assumed impermeable, with zero velocity conditions at domain edges. For flat-bed systems, velocities along the x- and y-axes are also zero.

Well boundary conditions account for hydrogen inflow, based on well geometry, formation permeability, and pressure gradient. A specific mass flow is imposed and pressure is computed to sustain it. The flow is evenly split among the four neighboring nodes. During extraction, the same logic applies with negative flow values; in equilibrium phases, pressures tend to equalize.

The simulation proceeds through discrete time steps, following this loop:

(i) Apply initial conditions;
(ii) Impose boundary conditions;
(iii) Generate the equation system;
(iv) Solve the system numerically;
(v) Update the pressure field;
(vi) Advance to the next time step and repeat.

The model also integrates gas composition dynamics. For each grid block, the mass fractions of gas components are calculated in tandem with pressure, based on a mass balance. Only incoming positive flows modify the block's composition, while outgoing flows retain their ratios and contribute to neighboring cells (Figure 2).

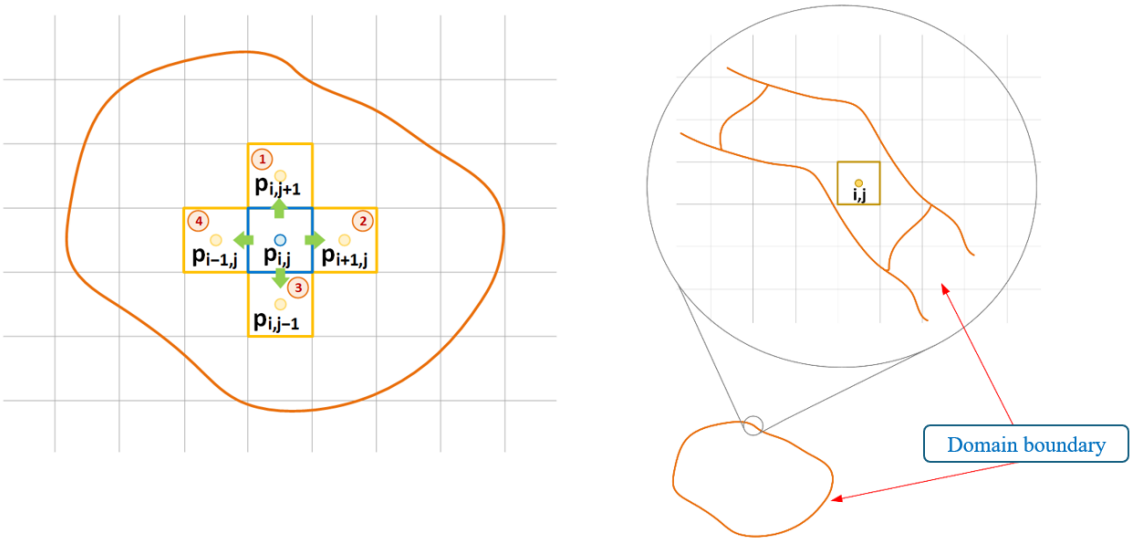

Figure 2. *Pressure condition diagram for a grid block and representation of blocks under boundary conditions*

To represent the reservoir geometry accurately, a digital domain map is created where each pixel is assigned attributes (boundary, well, internal/external cell). This enables automatic grid generation and targeted numerical calculations. During simulation, the domain map guides operations ensuring integration is performed only within active zones, with boundary and well conditions applied as needed.

RESULTS AND DISCUSSION

Four distinct simulation scenarios were analyzed to evaluate hydrogen injection behavior, pressure distribution, and diffusion dynamics within the studied depleted gas reservoir. In each scenario, a uniform daily volume of 250,000 Sm^3 of hydrogen was injected into each of the 15 wells over a 120 day period. This continuous injection phase was

subsequently followed by relaxation intervals of 5, 10, and 15 days, during which no gas was injected, allowing the system to reach local equilibrium. After each relaxation period, injection resumed at the same rate for an additional 30 day period, enabling assessment of how these resting intervals influenced pressure accumulation and gas dispersion.

Figure 3 illustrates the evolution of three key indicators over the 120-day continuous injection phase: the cumulative volume of injected hydrogen (Q), the average reservoir pressure (Pr), and the average wellbore pressure (Pw). The parameter Q shows a steady linear increase, reaching approximately 4.5×10^6 Sm³ by the end of the injection period. This linearity confirms that the injection rate was uniform and consistently maintained throughout the simulation. The Pr curve indicates a gradual increase in reservoir pressure from an initial value of around 30 bar to nearly 43 bar after 120 days. This smooth and near-linear progression reflects the reservoir's good pressure dissipation capacity, with no signs of localized overpressure.

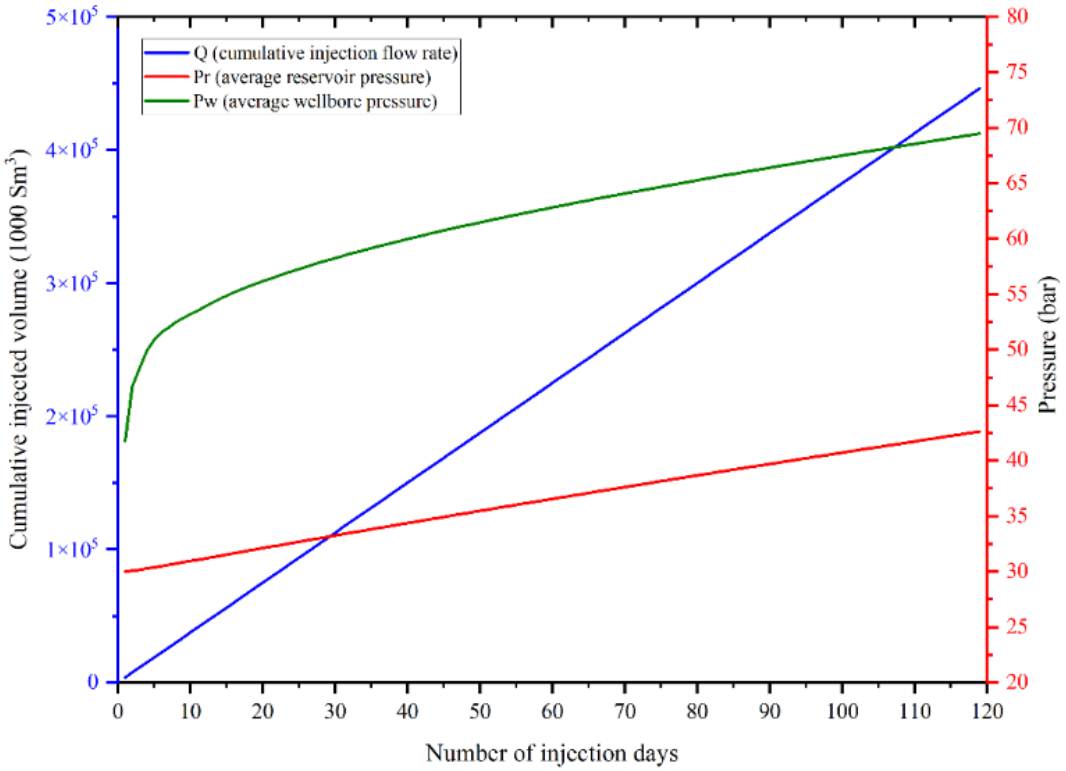

Figure 3. *Evolution of cumulative injected volume and average reservoir and wellbore pressures during a continuous injection period (120 days, 15 wells × 250,000)*

In contrast, the Pw curve representing average wellbore pressure displays a sharper rise during the first 20 days, followed by a plateauing trend between day 60 and day 120, peaking at approximately 70 bar. This behavior suggests that in the early phase, gas propagation encountered initial resistance near the well vicinity, leading to a rapid pressure increase. However, as local saturation progressed and preferential flow paths developed within the porous medium, the efficiency of gas injection improved and the pressure gradient began to stabilize.

The analyzed reservoir system exhibits stable behavior under continuous hydrogen injection, with no abrupt pressure spikes or signs of instability. This response suggests a favorable adaptation to constant injection regimes and indicates a low risk of fracture development or caprock integrity compromise under such operating conditions.

The difference observed between the average wellbore pressure (Pw) and the average reservoir pressure (Pr) emphasizes that the injection process is primarily influenced by localized entry resistance in the vicinity of the wells. However, the steady and progressive increase in Pr confirms the reservoir's capacity to gradually accommodate the injected gas, reflecting favorable petrophysical characteristics of the porous medium.

Notably, the post-injection relaxation period appears to have minimal influence on the analyzed parameters cumulative injected volume (Q), reservoir pressure (Pr), and wellbore pressure (Pw) in the second injection phase. This observation suggests that the system maintains robust performance regardless of pause interval length, indicating resilience against operational fluctuations.

Therefore, this scenario serves as a valuable benchmark for evaluating alternative injection strategies, particularly those incorporating post-injection relaxation intervals (5, 10, and 15 days). In such cases, pressure redistribution effects could play a significant role in determining storage efficiency and dynamic reservoir response.

Figure 4 presents the evolution of the cumulative injected hydrogen volume (Q), average reservoir pressure (Pr), and average wellbore pressure (Pw) during the second injection stage. This phase followed a pause of 5, 10, or 15 days, during which injection was temporarily halted to allow pressure redistribution and gas diffusion throughout the porous volume.

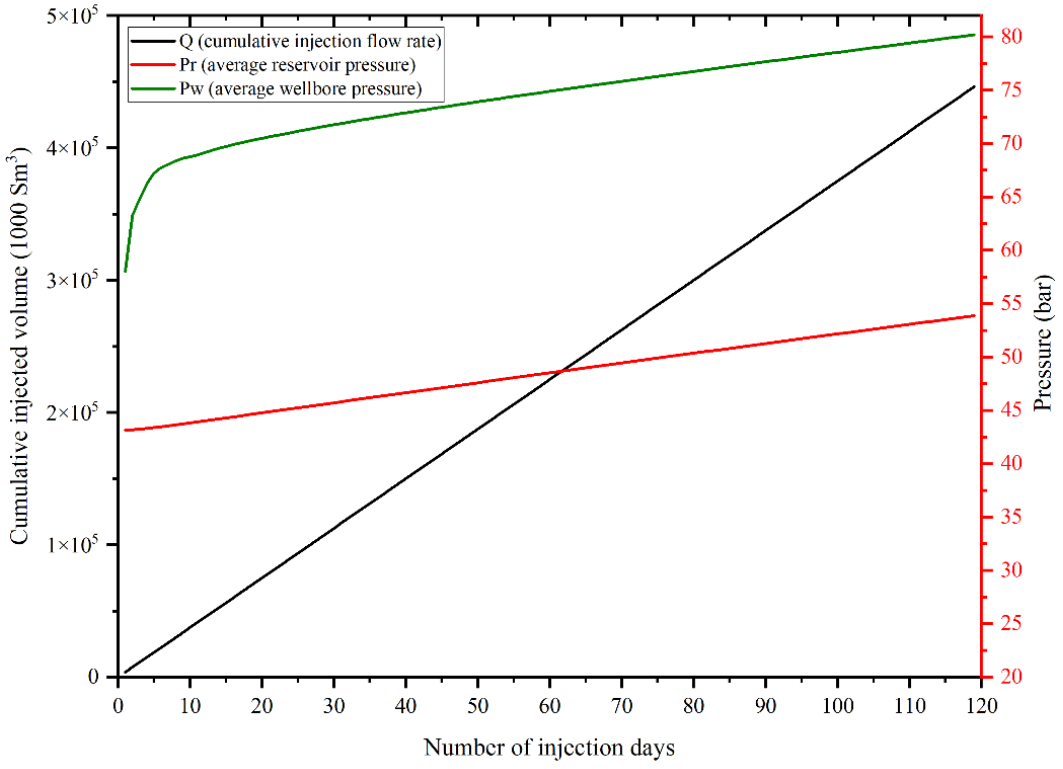

Figure 4. *Evolution of the cumulative volume of injected hydrogen and of the average pressures in the reservoir and in the well during the second injection phase, following the post-injection pause*

Compared to the previous figure (Figure 3 continuous injection over 120 days), several significant differences can be observed:

- The average reservoir pressure (Pr) starts from a higher initial value (approximately 43 bar, compared to 30 bar in the first phase), indicating that a portion of the pressure accumulated during the initial stage was retained in the system even after the relaxation period. This behavior suggests an effective hydrogen retention capacity within the porous medium.
- The average well pressure (Pw) reaches higher values and increases at a slightly accelerated rate compared to the first phase. This trend reflects increased resistance to injection during the second stage, likely due to partial saturation of the regions surrounding the wells or localized pressure buildup.
- The cumulative injected volume (Q) follows a similar linear trend as in the previous graph, but the slope of the curve is slightly lower. This implies a marginal decline in injection efficiency, potentially caused by the reduced compressibility of the medium already partially saturated with gas.

The second hydrogen injection phase, regardless of the duration of the post-injection pause (5, 10, or 15 days), reveals a coherent and predictable systemic behavior. A significant residual pressure is observed in the reservoir, indicating that the porous medium retains a substantial portion of the pressure accumulated during the initial stage, which directly influences the subsequent injection dynamics.

The average pressure in the well increases more sharply compared to the initial phase, suggesting a more rapid local accumulation of injected gas in the vicinity of the wells. This phenomenon may signal the need to optimize the injection–relaxation sequence to avoid localized overpressures or losses in injection efficiency.

At the same time, the evolution of the average reservoir pressure no longer follows a linear trend, but instead tends toward a quasi-stable regime. This behavior reflects the attainment of a threshold equilibrium regarding the capacity of the porous medium to accept additional gas under continuous injection conditions.

Therefore, this analysis provides a solid technical foundation for optimizing geological hydrogen storage strategies. The results emphasize the importance of relaxation stages in maintaining long-term system performance and support the development of balanced operational cycles that prevent reservoir degradation while maximizing injection efficiency. Table 1 highlights the differences in pressure evolution and system behavior for each scenario.

Table 1. *Comparison of reservoir behavior parameters between continuous injection and injection after a post-injection pause*

Parameter	Phase 1: Continuous Injection (120 days)	Phase 2: Injection after Pause
Initial reservoir pressure Pr (bar)	≈ 30	≈ 43
Initial well pressure Pw (bar)	≈ 40	≈ 58
Reservoir pressure evolution	Near-linear increase up to 43 bar	Near-linear increase up to 54 bar
Well pressure evolution	Rapid increase followed by plateau at ~70 bar	Accelerated increase exceeding 80 bar

Parameter	Phase 1: Continuous Injection (120 days)	Phase 2: Injection after Pause
Total injected volume Q (Nm^3)	$4.47 \cdot 10^6$ Sm^3	$4.47 \cdot 10^6$ Sm^3
System tendency	Stable response, no abrupt accumulation	High residual pressure with a stiffer system response

Figure 5 illustrates the evolution of pressure distribution (30–75 bar) and volumetric hydrogen saturation (5–100%) within the two-dimensional reservoir model at four key timepoints: immediately after injection and following relaxation periods of 5, 10, and 15 days. The pressure distribution (images a1–a4) initially reveals high accumulation around the wells, with local pressures reaching peak values of 65–75 bar. This overpressure zone appears compact immediately after injection (a1). As the relaxation time increases (a2 to a4), a gradual dissipation of pressure is observed, with the medium-pressure zones extending toward the reservoir periphery. This trend suggests a natural tendency toward isobaric equilibration within the porous medium, contributing to a more uniform redistribution of the injected gas. In parallel, images b1–b4 depict the volumetric diffusion of hydrogen throughout the reservoir during the relaxation periods. Immediately after injection (b1), maximum saturation (100%) is concentrated near the wells. After 5 days (b2), the saturated zones expand and are accompanied by regions of intermediate saturation (50–90%). By day 10 (b3), hydrogen has penetrated deeper into the porous structure, covering a larger area and reaching more distant regions. After 15 days (b4), the saturation becomes significantly more dispersed and homogeneous, indicating an advanced diffusion regime and the approach of a volumetric equilibrium state.

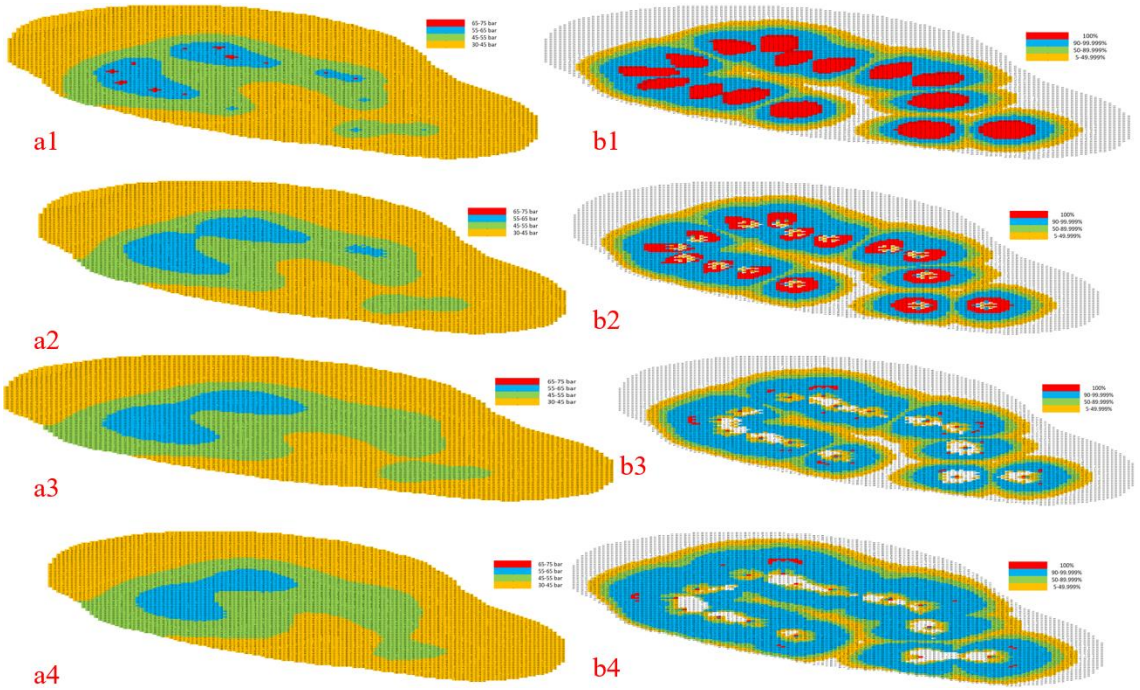

Figure 5. *Distribution of pressure (30–88 bar) and volumetric hydrogen saturation (5–100%) in the reservoir after the second injection phase results obtained through numerical simulation: (a5 and b5) after a 5-day relaxation period, (a6 and b6) after 10 days of relaxation, and (a7 and b7) after 15 days of relaxation.*

These observations confirm that longer relaxation periods enable a more efficient redistribution of the injected gas, reduce excessive local pressures, and enhance the overall storage efficiency. The results are consistent with the findings reported in the literature, where similar behaviors were observed using simulations conducted with the H_2Storage simulator [25,26]. Clearly, pressure dynamics directly influence hydrogen migration and retention within the porous medium, highlighting the importance of relaxation stages in optimizing injection cycle performance.

Figure 6 illustrates the evolution of pressure distribution (30–88 bar) and volumetric hydrogen saturation (5–100%) within the reservoir following the second injection phase, conducted after relaxation periods of 5, 10, and 15 days. Interestingly, the pressure distribution maps (a5–a7) reveal no significant differences among the analyzed cases. In all three scenarios, overpressure zones (75–88 bar) remain extensive and concentrated around the injection wells, indicating a consistent pattern of localized accumulation regardless of the relaxation duration applied beforehand.

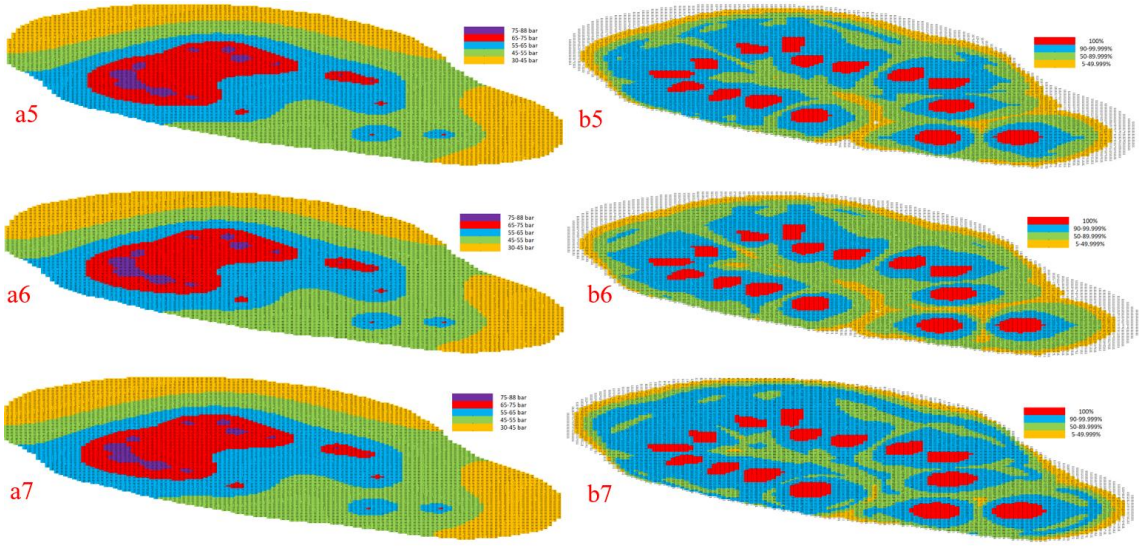

***Figure 6**. Distribution of pressure (30–88 bar) and volumetric hydrogen saturation (5–100%) within the two-dimensional reservoir model – results obtained through numerical simulation: (a5 and b5) injection after 5 days of relaxation, (a6 and b6) injection after 10 days of relaxation, and (a7 and b7) injection after 15 days of relaxation.*

In contrast, the analysis of hydrogen saturation distribution (b5–b7) highlights clear differences in the diffusion behavior of the gas. After 5 and 10 days of relaxation (b5 and b6), saturation remains predominantly confined around the wells, with limited propagation into the porous medium. However, in the 15-day relaxation scenario (b7), hydrogen diffuses more effectively throughout the reservoir, with intermediate saturation zones (50–90%) becoming more widespread and the overall distribution appearing significantly more homogeneous. This indicates that the system was given sufficient time to redistribute internal pressure and facilitate the migration of gas toward the peripheral regions of the storage formation.

This observation suggests that, despite the relatively unchanged global pressure profiles across the three cases, efficient hydrogen diffusion into the porous matrix is achieved only when an extended relaxation period is allowed. Therefore, a 15-day relaxation

interval plays a critical role not only in mitigating excessive local pressure buildup but also in enhancing the effective utilization of the available pore space for gas storage.

Moreover, the limited diffusion observed in the shorter relaxation scenarios (5 and 10 days) increases the risk of local pressure accumulation, which, under real operating conditions, could threaten the structural integrity of the reservoir. Thus, the distribution shown in panel b7 indirectly confirms that optimizing the duration of the relaxation stage is essential for ensuring operational safety and maximizing the actual hydrogen storage capacity.

CONCLUSIONS

The conducted numerical simulations provide compelling evidence of the dynamic behavior of hydrogen injection in porous media under varying operational strategies**.** Specifically, continuous hydrogen injection over a prolonged period (120 days) resulted in a stable and predictable reservoir response, characterized by a near-linear increase in reservoir pressure and a plateauing trend in wellbore pressure. This behavior confirms the ability of the porous medium to accommodate significant volumes of injected gas without inducing structural failures or pressure-driven fracturing.

By contrast, the inclusion of post-injection relaxation intervals (5, 10, and 15 days) introduced notable variations in pressure redistribution and hydrogen saturation behavior. Shorter pauses (5–10 days) yielded limited gas diffusion and localized pressure buildup near injection wells. However, the 15-day relaxation scenario enabled deeper hydrogen penetration, expansion of intermediate saturation zones, and a more uniform distribution of gas across the reservoir domain. This indicates that extended pauses allow the system to approach a quasi-equilibrium state, ultimately improving both storage efficiency and operational safety.

Crucially, while the global pressure profiles appear similar across all cases, substantial differences emerge in the saturation patterns and pore space utilization. This underscores the inadequacy of relying solely on pressure metrics when assessing storage performance. Instead, a more comprehensive evaluation that incorporates diffusive transport and spatial gas redistribution is necessary for optimizing injection strategies.

In conclusion, this study demonstrates that the adoption of tailored injection–relaxation cycles is vital for enhancing underground hydrogen storage performance. The 15-day relaxation interval proved particularly effective, striking a balance between diffusion efficiency and system stability. These results not only reinforce findings from prior simulation studies and provide actionable insights for the large-scale implementation of safe and efficient hydrogen storage protocols in depleted gas reservoirs, but also provide a clear basis for future field-scale validation and methodological refinement.

REFERENCES

1. Muhammed, N.S.; Haq, B.; Al Shehri, D.; Al-Ahmed, A.; Rahman, M.M.; Zaman, E., A review on underground hydrogen storage: Insight into geological sites, influencing factors and future outlook. *Energy Reports* 2022, *8*, 461-499, doi:https://doi.org/10.1016/j.egyr.2021.12.002.

2. Quintos Fuentes, J.E.; Santos, D.M.F., Technical and Economic Viability of Underground Hydrogen Storage. *Hydrogen* 2023, *4*, 975-1000, doi:10.3390/hydrogen4040057.
3. Bade, S.O.; Taiwo, K.; Ndulue, U.F.; Tomomewo, O.S.; Aisosa Oni, B., A review of underground hydrogen storage systems: Current status, modeling approaches, challenges, and future prospective. *International Journal of Hydrogen Energy* 2024, *80*, 449-474, doi:https://doi.org/10.1016/j.ijhydene.2024.07.187.
4. Lysyy, M.; Føyen, T.; Johannesen, E.B.; Fernø, M.; Ersland, G., Hydrogen Relative Permeability Hysteresis in Underground Storage. *Geophysical Research Letters* 2022, *49*, e2022GL100364, doi:https://doi.org/10.1029/2022GL100364.
5. Hagemann, B.; Rasoulzadeh, M.; Panfilov, M.; Ganzer, L.; Reitenbach, V., Hydrogenization of underground storage of natural gas. *Computational Geosciences* 2016, *20*, 595-606, doi:10.1007/s10596-015-9515-6.
6. Abdellatif, M.; Azizmohammadi, S.; Stiedl, G.; Pichler, M.; Ott, H., Sensitivity analysis of the methanation process in underground hydrogen storage: A case study in Upper Austria. *International Journal of Hydrogen Energy* 2025, *105*, 1164-1177, doi:https://doi.org/10.1016/j.ijhydene.2025.01.381.
7. Feldmann, F.; Hagemann, B.; Ganzer, L.; Panfilov, M., Numerical simulation of hydrodynamic and gas mixing processes in underground hydrogen storages. *Environmental Earth Sciences* 2016, *75*, 1165, doi:10.1007/s12665-016-5948-z.
8. Shirzad, G.; Shirkhani, A.; Hoseinzadeh, S., Underground hydrogen storage in naturally fractured reservoirs: Matrix scale modeling for cushion gas selection. *International Journal of Hydrogen Energy* 2025, *116*, 266-278, doi:https://doi.org/10.1016/j.ijhydene.2025.03.052.
9. Pfeiffer, W.T.; al Hagrey, S.A.; Köhn, D.; Rabbel, W.; Bauer, S., Porous media hydrogen storage at a synthetic, heterogeneous field site: numerical simulation of storage operation and geophysical monitoring. *Environmental Earth Sciences* 2016, *75*, 1177, doi:10.1007/s12665-016-5958-x.
10. Luboń, K.; Tarkowski, R., Numerical simulation of hydrogen injection and withdrawal to and from a deep aquifer in NW Poland. *International Journal of Hydrogen Energy* 2020, *45*, 2068-2083, doi:https://doi.org/10.1016/j.ijhydene.2019.11.055.
11. Cai, Z.; Zhang, K.; Guo, C., Development of a novel simulator for modelling underground hydrogen and gas mixture storage. *International Journal of Hydrogen Energy* 2022, *47*, 8929-8942, doi:https://doi.org/10.1016/j.ijhydene.2021.12.224.
12. Lucena, S.M.P.; Casacão, J.; Althoff, H.; Ribeiro, C.; Castro, J.V.; Silvino, P.; Rodrigues, L.G., Impact of different cushion gases (CO2, CH4 and N2) and cycles in a brazilian equatorial margin oil field converted to H2 storage. *International Journal of Hydrogen Energy* 2025, doi:https://doi.org/10.1016/j.ijhydene.2025.02.313.
13. Salmachi, A.; Seyfaee, A.; Robert, R.J.; Hosseini, T.; Nathan, G.; Ashman, P.; Roberts, A.; Jafarian, M.; Simon, C., Underground hydrogen storage: Integrated surface facilities and fluid flow modelling for depleted gas reservoirs. *International Journal of Hydrogen Energy* 2024, *50*, 1055-1069, doi:https://doi.org/10.1016/j.ijhydene.2023.08.335.

14. Saadat, Z.; Farazmand, M.; Sameti, M., Integration of underground green hydrogen storage in hybrid energy generation. *Fuel* 2024, *371*, 131899, doi:https://doi.org/10.1016/j.fuel.2024.131899.
15. Sainz-Garcia, A.; Abarca, E.; Rubi, V.; Grandia, F., Assessment of feasible strategies for seasonal underground hydrogen storage in a saline aquifer. *International Journal of Hydrogen Energy* 2017, *42*, 16657-16666, doi:https://doi.org/10.1016/j.ijhydene.2017.05.076.
16. Saeed, M.; Jadhawar, P.. Modelling underground hydrogen storage: A state-of-the-art review of fundamental approaches and findings. *Gas Science and Engineering* 2024, *121*, 205196, doi:https://doi.org/10.1016/j.jgsce.2023.205196.
17. Lysyy, M.; Fernø, M.; Ersland, G., Seasonal hydrogen storage in a depleted oil and gas field. *International Journal of Hydrogen Energy* 2021, *46*, 25160-25174, doi:https://doi.org/10.1016/j.ijhydene.2021.05.030.
18. Pfeiffer, W.T.; Bauer, S., Subsurface Porous Media Hydrogen Storage – Scenario Development and Simulation. *Energy Procedia* 2015, *76*, 565-572, doi:https://doi.org/10.1016/j.egypro.2015.07.872.
19. Mahdi, D.; Al-Khdheeawi, E.; Yuan, Y.; Zhang, Y.; Iglauer, S., Hydrogen underground storage efficiency in a heterogeneous sandstone reservoir. *Advances in Geo-Energy Research* 2021, *5*, 437-443, doi:10.46690/ager.2021.04.08.
20. Jadhawar, P.; Saeed, M., Optimizing the operational efficiency of the underground hydrogen storage scheme in a deep North Sea aquifer through compositional simulations. *Journal of Energy Storage* 2023, *73*, 108832, doi:https://doi.org/10.1016/j.est.2023.108832.
21. Eparu, C.N.; Prundurel, A.P.; Doukeh, R.; Stoica, D.B.; Ghețiu, I.V.; Suditu, S.; Stan, I.G.; Rădulescu, R., Optimizing Underground Natural Gas Storage Capacity through Numerical Modeling and Strategic Well Placement. *Processes* 2024, *12*, doi:10.3390/pr12102136.
22. Eparu, C.N.; Suditu, S.; Doukeh, R.; Stoica, D.B.; Ghețiu, I.V.; Prundurel, A.; Stan, I.G.; Dumitrache, L., Software for CO2 Storage in Natural Gas Reservoirs. *Energies* 2024, *17*, doi:10.3390/en17194984.
23. Du Fort, E.C.; Frankel, S.P., Stability Conditions in the Numerical Treatment of Parabolic Differential Equations. *Mathematical Tables and Other Aids to Computation* 1953, *7*, 135-152, doi:10.2307/2002754.
24. Chen, Z.; Huan, G.; Ma, Y., Computational Methods for Multiphase Flows in Porous Media. *Society for Industrial and Applied Mathematics* 2006, *2*, doi:10.1137/1.9780898718942.
25. Jadhawar, P.; Saeed, M., Mechanistic evaluation of the reservoir engineering performance for the underground hydrogen storage in a deep North Sea aquifer. *International Journal of Hydrogen Energy* 2024, *50*, 558-574, doi:https://doi.org/10.1016/j.ijhydene.2023.07.272.
26. Arekhov, V.; Clemens, T.; Wegner, J.; Abdelmoula, M.; Manai, T., The Role of Diffusion on Reservoir Performance in Underground Hydrogen Storage. *SPE Reservoir Evaluation & Engineering* 2023, *26*, 1566-1582, doi:10.2118/214435-PA.

Received: November 2025; Revised: December 2025; Accepted: December 2025; Published: December 2025